

Molecular dynamics studies of Lithium intercalation into amorphous nanostructure of Titanium dioxide.

¹M. G. Matshaba, ²D. C. Sayle and ¹P. E. Ngoepe

¹Materials Modelling Centre, School of Physical and Mineral Sciences, University of Limpopo, Private Bag X 1106, Sovenga, 0727, South Africa.

²School of Physical Sciences, University of Kent, Canterbury, Kent, CT2 7NZ, United Kingdom.

E-mail: malili.matshaba@ul.ac.za

Abstract. Titanium dioxide (TiO₂) has been confirmed as a safe anode material in lithium ion batteries due to its higher Li-insertion potential, (1.5V) in comparison with commercialised carbon anode materials. Besides being used as an anode material it has a wide range of applications such as photo-catalysis, insulators in metal oxide, dye sensitized solar cells etc. In this work amorphous nanostructure of TiO₂ comprising of 15972 atoms was lithiated with a different concentration of lithium atoms. Simulation of amorphisation and re-crystallisation was employed to attain Li-TiO₂ nanostructures and its microstructures. Molecular dynamics has been performed to crystallise intercalated nanostructure using the computer code DL_Poly. The crystallisation of the materials, starting from amorphous precursors, and the complex microstructure of the material was captured within each structural model including: polymorphic rutile and brookite structures, dislocations, grain boundaries, micro-twinning, vacancies, interstitials, surfaces and morphology. Microstructure depict the lithium atoms situated on the tunnels and vacancies, shows that the material can store and transport lithium during charging and discharging, making it an attractive anode material. Calculated X-Ray diffractions are in accord with the experimental data revealing the presence of brookite and rutile phases.

1. Introduction

The TiO₂ is one of the most extensively studied metal oxide and has been widely used in photocatalysis [1], photosplitting of water [2], photochromic devices [3], gas sensing, dye-sensitized solar cells (DSSCs) (energy conversion) [4] and rechargeable lithium ion batteries (LIBs) (electrochemical storage) [5 - 12]. Over the last two decades, the increasing demand of energy and shifting to the renewable energy resources, has rendered LIBs to be considered as promising alternative and green technology for energy storage applied in hybrid electric vehicles (HEVs), plug-in hybrid electric vehicles (PHEVs), and other electric utilities. TiO₂ is being considered as one of the most attractive anode materials of LIBs owing to the following distinct characteristics: (i) its potential vs. Li^o (~1.5-1.7 V) prevents the plating of metallic lithium at the negative electrode, thus enhancing the safety and extending the life of the cell, (ii) it exhibits relatively high practical capacity (~200 mAh/g), certainly smaller than graphite, but greater than its lithiated form Li₄Ti₅O₁₂, and (iii) it is environmentally benign, abundant, inexpensive and has stable structure. Its most significant advantage, however, is the ability to be charged and discharged at a high current rate (high power). The above-mentioned points are of great importance since large-scale batteries for hybrid electric vehicles and other applications require prolonged life,

improved safety, and reduced cost. In general, the properties of TiO₂ greatly depend on the crystal sizes, phases, exposed facets, and morphologies. We now consider lithium insertion in nanoparticle of anatase TiO₂, which as the size of TiO₂ falls in the nanometers, tends to be more stable than other polymorphs, owing to differences in particle surface tension, size, and shape. A larger Li-ion conductivity is deduced from simulation results for particle size smaller than 20 nm, and lower conductivity for larger nanoparticles.

Simulation of amorphisation and re-crystallisation was employed to attain Li-TiO₂ using the DL_POLY code[13]. We have lithiated nanostructure of TiO₂ with 50 Li atoms. Lithiated nanostructure of TiO₂ is presented in figure 1 below. Charge compensation in the structure is achieved by changing the titanium (4+ oxidation state) closest to the lithium cation into the Jahn-Teller active titanium (3+ oxidation state). This process is repeated for all the lithium ions inserted in the structure.

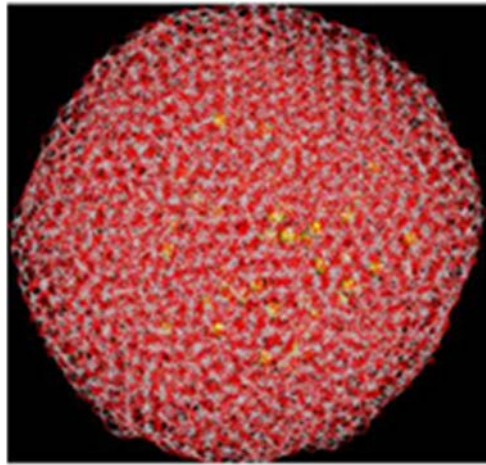


Figure 1. Lithiated amorphous nanostructure of TiO₂ with 50 Li atoms

2. Methodology

The Calculations are based on the Born model of ionic solids, where Ti⁴⁺, Ti³⁺, Li⁺ and O²⁻ ions interact via long-range Coulomb and short range interactions interact via long-range Coulomb and short range interactions. The potentials used in this study were optimized by Matsui [14] for the four polymorphs of TiO₂ (rutile, anatase, brookite and TiO₂ II [α -PbO₂ structure]), and are presented in table 1. The short range interactions are described by Buckingham potentials and the interaction energy takes the form

$$U_{ij} = \frac{q_i q_j}{4\pi\epsilon\epsilon_0 r_{ij}} + A_{ij} \exp\left(-\frac{r_{ij}}{\rho_{ij}}\right) - \frac{C_{ij}}{r_{ij}}$$

Where A_{ij} is the size of the ions, ρ_{ij} is the hardness and C_{ij} is the dispersion parameter. The repulsive interaction between the ions is represented by the first term while the second term is the van der Waals attractive interaction of the ions. All the molecular dynamics simulations were performed using DL_POLY code [13].

Table 1 Buckingham potentials used for lithiated TiO₂

Ion pair (ij)	A _{ij} (eV)	ρ_{ij} (Å)	C _{ij} (eV.Å ⁶)
Ti ³⁺ -O ²⁻	18645.840	0.1950	22.0000
Li ⁺ -O ²⁻	426.48000	0.3000	0.00000
Ti ³⁺ -Ti ⁴⁺	28707.210	0.1560	16.0000
Ti ³⁺ -Ti ³⁺	33883.920	0.1560	16.0000

3. Results and discussion

Lithiated nanostructure of TiO₂ was recrystallised, from the plot of configuration energy which is depicted in figure 2 shows that the nanostructure with lithium atoms has recrystallised. The change of the configuration energy from -2.015×10^5 to -2.043×10^5 eV corresponds to the latent heat of crystallisation and is associated with the transition from an amorphous to a crystalline phase. Beyond 0.6 ns the change in the configuration energy is very small, which indicates that the nanosphere has recrystallised. At 2 ns the energy starts to be near constant which reveals that complete recrystallisation has been achieved.

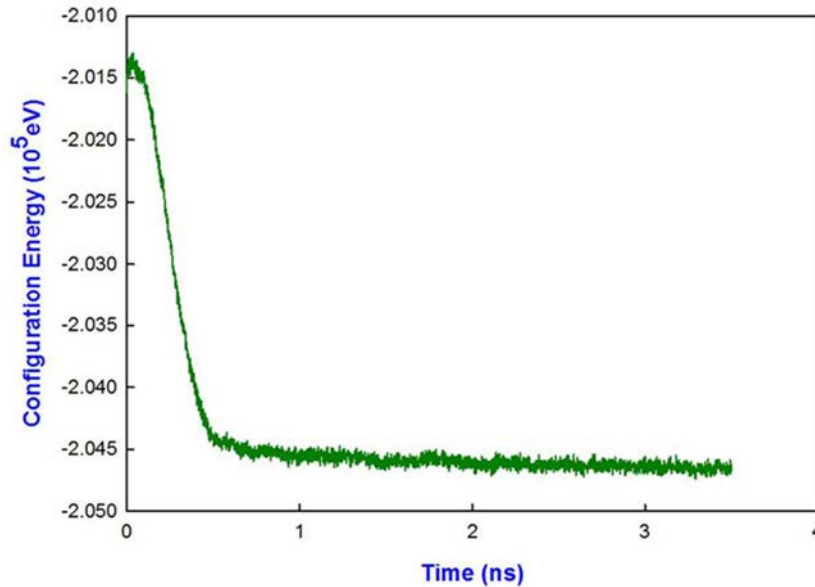


Figure 2. Calculated configuration energy as a function of time for the lithiated nanostructure of TiO₂.

As crystallisation occurs some lithium atoms move out of the nanostructure or away. Our simulation technique divulge that lithium atoms can move away from the nanostructure half the diameter of the nanostructure. Lithium atoms that have moved out of the nanostructure will be captured in electrolyte then transported to cathode material. Recrystallised nanostructure of TiO₂ is depicted in figure 3. Clear patterns are observed on the structure indicating that the nanostructure is recrystallised. We cooled the recrystallised nanostructure gradually by firstly performing MD simulations for 500 ps at temperature of 1500 K, followed by a run for 250 ps at 1000 K, and lastly for 500 ps at temperature of 0 K. Cooled nanostructure of TiO₂ with 50 lithium atoms is shown in figure 3,

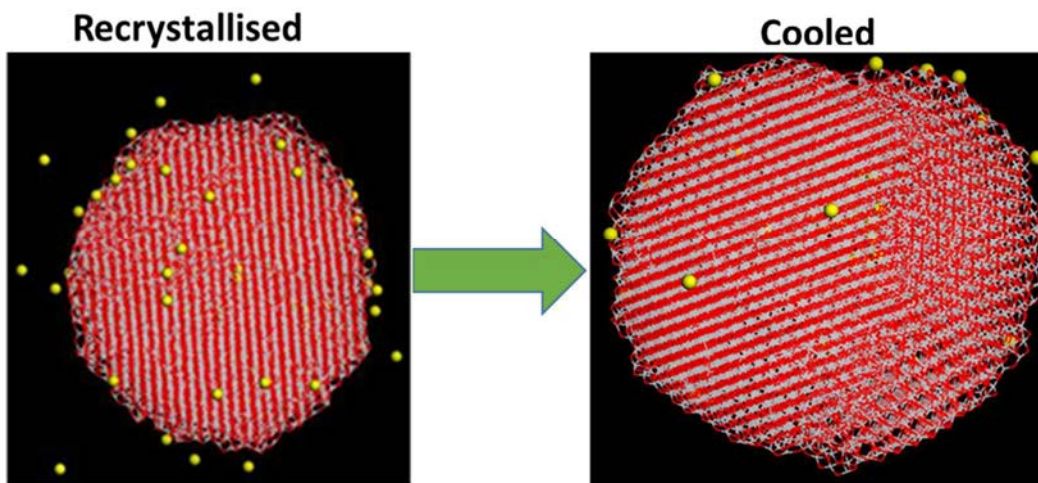


Figure 3. Recrystallised and cooled nanostructure of lithiated TiO₂.

Microstructure was created in order to analyse the positions of lithium atoms inside the nanostructure. The microstructure of nanoparticle of TiO_2 is depicted in figure 4. The blue octahedra correspond to the upper layer of Ti^{4+} , and the white adjacent the lower layer and the lithium atoms are represented by yellow balls. The microstructure of the nanostructure shows zigzag tunnels which are associated with the brookite and the straight tunnels that are related to the twinned rutile polymorphs. Few vacancies are observed on the microstructure, and lithium atoms have moved into vacancies of the structure. A good anode requires the nanostructure to store optimum lithium atoms and provide pathways for their transport. Indeed the microstructure of the nanoparticle reflects lithium atoms that are located in the tunnels. A few lithium atoms are located at the edges of the system and those in the nanostructure are positioned in tunnels and have filled existing vacancies.

Simulated X-Ray diffractions depicted in figure 5 shows picks that accord to rutile and brookite polymorphs as compared with the experimental picks [15]. Two peaks just below and above 30° accord with the brookite and $\text{TiO}_2: \alpha\text{-PbO}_2$ structures. At 37° and 57° , observed peaks correspond to all measured structures. Simulated XRDs at 50° has a smooth curve which accords with the rutile structure. At 67° we notice a peak which is in agreement with $\text{TiO}_2: \alpha\text{-PbO}_2$ and rutile polymorphs. This implies that the lithiated TiO_2 nanostructure has a combination of brookite, $\text{TiO}_2: \alpha\text{-PbO}_2$ and rutile structural arrangements.

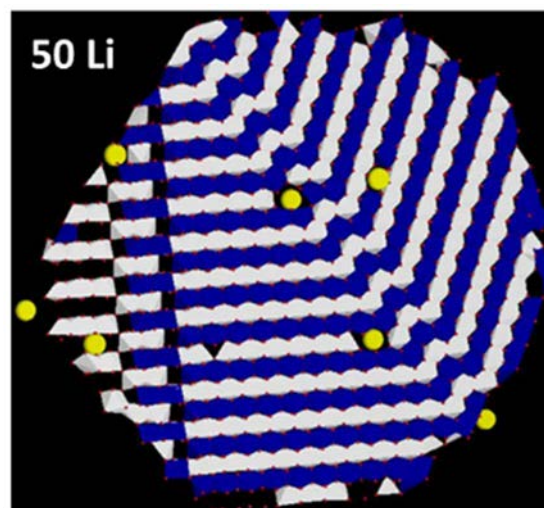


Figure 4. Microstructure of nanostructure of TiO_2 with 50 Li atoms.

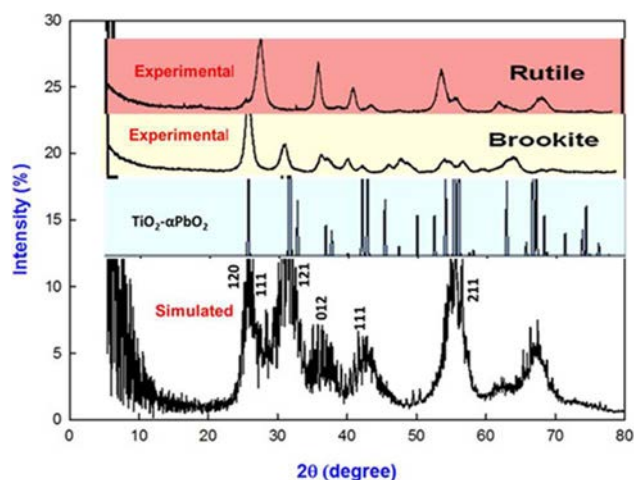


Figure 5. A comparison simulated TiO_2 nanostructure with calculated $\text{TiO}_2: \alpha\text{-PbO}_2$ and experimental [15] XRDs.

4. Conclusion

Amorphisation and recrystallisation technique has been successfully employed to generate nanostructures of TiO₂ with 50 Li atoms. The change of the configuration energy shows an amorphise-crystalline transition and can estimate the latent heat of crystallisation. Their XRDs confirm a brookite structural arrangement and they are accord with those of TiO₂: α -PbO₂. Microstructures of simulated nanostructure concur well on types of TiO₂ polymorphs that are present. Nanostructure of TiO₂ confirms a good anode material.

Acknowledgements

Calculations were performed at Materials Modelling Centre (MMC), University of Limpopo. This work is supported by Department of Science and Technology, National Research Foundation, Pretoria, the Department of Science and Technology HySA Lithium Ion Batteries and Supercapacitors Project, Pretoria and the Centre for High Performance Computing (CHPC) in South Africa.

References

- [1] Schneider J, Matsuoka M, Takeuchi M, Zhang J, Horiuchi Y, Anpo M and Bahnemann D W 2014 *Chem. Rev.* **114** (19) 9919-9986.
- [2] Ni M, Leung M K H, Leung D Y C and Sumathy K A 2007 *Renew. Sust. Energ Rev* **11** (3) 401-425.
- [3] Biancardo M, Argazzi R and Bignozzi C 2005 *Inorg. Chem.* **44** (26) 9619-9621.
- [4] Liu B and Aydil E S 2009 *J. Am. Chem. Soc.* **131** (11) 3985-3990.
- [5] Fujishima A and Honda K 1972 *Nature* **238** 37-38.
- [6] O'Regan B and Gratzel M. 1991 *Nature* **353** 737-740.
- [7] Chen X and Mao S S 2007 *Chem. Rev.* **107** 2891-2959.
- [8] Liu, B, Deng D, Lee J Y and Aydil E S 2010 *J. Mater. Res.* **25** (8) 1588-1594.
- [9] Liu H, Bi Z, Sun X-G, Unocic R R, Paranthaman M P, Dai S and Brown G M 2011 *Adv. Mater.* **23** 3450-3454.
- [10] Liu S, Li J, Shen Q, Cao Y, Guo X, Zhang G, Feng C, Zhang J, Liu Z, Steigerwald M L, Xu D and Nuckolls C 2009 *Angew. Chem. Int. Ed.* **48**, 4759-4762.
- [11] Trascon J M and Armand M 2001 *Nature* 2001 **414** 359-367.
- [12] Wakihara W and Yamamoto O 1998 Wiley-VCH 181-198.
- [13] Smith W and Forster T R. 1996. <http://www.dl.ac.uk/TCSC/Software/DLPOLY>.
- [14] Matsui M and Akaogi M 1991 *Mol. simul.* **6** 239-244.
- [15] Dambournet D Belharouak I and Amine K 2009 *Electrochem. Soc.* 215, No.1.